ADVANCED MATERIALS TECHNOLOGIES
www.advmattechnol.de

Biocompatible and Highly Stretchable PVA/AgNWs Hydrogel Strain Sensors for Human Motion Detection

*Shohreh Azadi, Shuhua Peng, Sajad A. Moshizi, Mohsen Asadnia, Jiangtao Xu, Inkyu Park, Chun H. Wang, and Shuying Wu**

Hydrogel-based strain sensors have attracted considerable interest for applications such as skin-like electronics for human motion detection, soft robotics, and human–machine interfaces. However, fabrication of hydrogel strain sensors with desirable mechanical and piezoresistive properties is still challenging. Herein, a biocompatible hydrogel sensor is presented, which is made of polyvinyl alcohol (PVA) nanocomposite with high stretchability up to 500% strain, high mechanical strength of 900 kPa, and electrical conductivity (1.85 S m^{-1}) comparable to human skin. The hydrogel sensors demonstrate excellent linearity in the whole detection range and great durability under cyclic loading with low hysteresis of 7%. These excellent properties are believed to be contributed by a new bilayer structural design, i.e., a thin, conductive hybrid layer of PVA/silver nanowires (AgNWs) deposited on a pure strong PVA substrate. PVA solution of high concentration is used to fabricate the substrate while the top layer consists of dilute PVA solution so that high content of AgNWs can be dispersed to achieve high electrical conductivity. Together with a rapid response time (0.32 s) and biocompatibility, this new sensor offers great potential as a wearable sensor for epidermal sensing applications, e.g., detecting human joint and muscle movements.

1. Introduction

Flexible and stretchable sensors are attracting significant interest in a wide range of applications including health monitoring, diagnostic devices, soft robotics, and electronic skins.[1–6] Piezoresistive sensors, one of the main types of sensors, change their resistance in response to mechanical deformation and have demonstrated a number of applications in monitoring strain,[4–8] pressure,[6,7,9] flow,[10–12] and temperature.[4,13,14] To meet the requirements for both human motion detection and biosafety, flexible sensors should be biocompatible. In this regard, different types of elastomers such as polydimethylsiloxane (PDMS) or hydrogels such as polyvinyl alcohol (PVA) hydrogels have been extensively used as the flexible substrate/matrix.[15–18] While the flexible substrate/matrix, in most cases, determines the mechanical properties of the sensors, conductive materials including carbon nanoparticles,[6] carbon nanofibers (CNFs),[15,19] carbon nanotubes (CNTs),[20] graphene,[5,21] silver nanowires (AgNWs),[19,22] and silver nanoparticles[23] have been successfully used as the sensing elements. Different techniques have been developed to incorporate conductive elements with the flexible substrate/matrix. For instance, direct mixing of polymeric components with conductive nanomaterials has been extensively studied.[4,16,24] More recently, dip-coating/spin-coating and in situ polymerization have been utilized to develop conductive composite sensors with porous structure,[15] double layer or sandwich structures.[4,25]

Among different types of flexible sensors, hydrogel-based sensors have gained increasing interest in recent years due to their human tissue-like mechanical properties and excellent biocompatibility. Different types of hydrogel sensors have been demonstrated recently, including composite hydrogels containing conductive nanomaterials[16,17] or conducting polymers (e.g., polyaniline),[26] ionic conductive hydrogels,[25] as well as zwitterionic hydrogel sensors.[27] PVA is a promising candidate for wearable applications where biocompatibility is required.[16,28] Research into the fabrication of PVA-based hydrogel sensors currently focuses on the relationship between the mechanical properties and material design factors such as PVA concentration, preparation process, and the incorporation of conductive nanofillers.[29,30] However, adding crosslinking agents and conductive nanomaterials can affect the mechanical properties of PVA hydrogels. Cai et al. presented an extremely stretchable strain sensor based on PVA, CNTs, and borax, which exhibited a high stretchability of up to 1000% strain with

S. Azadi, S. A. Moshizi, Dr. M. Asadnia, Dr. S. Wu
School of Engineering
Macquarie University Sydney
Sydney, NSW 2109, Australia
E-mail: shuying.wu@mq.edu.au
Dr. S. Peng, Prof. C. H. Wang, Dr. S. Wu
School of Mechanical and Manufacturing Engineering
University of New South Wales
Sydney, NSW 2052, Australia
Dr. J. Xu
School of Chemical Engineering
University of New South Wales
Sydney, NSW 2052, Australia
Prof. I. Park
Department of Mechanical Engineering
Korea Advanced Institute of Science and Technology (KAIST)
Daejeon 34141, South Korea
The ORCID identification number(s) for the author(s) of this article can be found under https://doi.org/10.1002/admt.202000426.

DOI: 10.1002/admt.202000426

rapid self-healing properties and high sensitivity.[16] Liao et al. developed a wearable epidermal sensor based on single-wall CNTs, PVA, and polydopamine.[31] Their sensors revealed moderate sensing performance along with low cytotoxicity, which demonstrated the promising potential of PVA-based sensors in applications such as health monitoring and therapy.

One of the major challenges in developing PVA-based nanocomposite hydrogel sensors is to find a method to properly incorporate the conductive nanomaterials to achieve desirable mechanical strength and electrical conductivity. While high concentration of PVA is critical to attain high mechanical strength, conductive nanomaterials can be better dispersed in low concentration PVA solution as concentrated solution is very viscous. To overcome this issue, herein, we developed a PVA/AgNWs hydrogel strain sensor with a new structural design, i.e., a bilayer structure having a thin, highly conductive PVA/AgNWs layer supported by a strong PVA substrate layer. The bottom layer is made of high concentration PVA and thereby is mechanically strong while the top layer is from much more dilute PVA solution so that high content of AgNWs can be dispersed to achieve high electrical conductivity. The new structural design reported in this work simultaneously endows the strain sensors with both desirable electric conductivity and high mechanical strength. Freezing–thawing method was employed, during which crystallization of PVA occurs and the resulted crystallites act as physical cross-links to establish the strong network in the PVA hydrogel.[29] The present study also demonstrates that, by varying the PVA concentration in the supporting substrate and the concentration of AgNWs in the sensing layer, their mechanical properties and sensing performance can be tuned. Finally, the biocompatibility was examined, and its potentials in detecting human joint movements and facial expression were demonstrated.

2. Experimental Section

2.1. Materials

PVA ($M_w \approx 89\,000$), polyvinylpyrrolidone (PVP, $M_w \approx 40\,000$), $AgNO_3$ powder, and sodium chloride (NaCl) powder were purchased from Sigma Aldrich. Glycerol was obtained from Chem-Supply. Normal human fibroblasts (NHF) were purchased from Lonza, Inc. Cell culture materials including Dulbecco's modified Eagle medium (DMEM), fetal bovine serum (FBS), trypsin, and phosphate buffered saline (PBS) were purchased from Thermo Fisher Scientific.

2.2. Synthesis of AgNWs

AgNWs were synthesized according to a previously published method.[32] Briefly, 5.86 g of PVP was dissolved into 190 mL of glycerol and heated to 90 °C. Then 1.58 g of $AgNO_3$ powder was added to the solution followed by adding a mixture of 10 mL glycerol, 59 mg NaCl, and 0.5 mL H_2O. The solution was heated up to 200 °C and stirred at 50 rpm until the color of the solution changed to gray-green, indicating the formation of AgNWs. Afterward, the reaction was stopped by adding large quantity of deionized water. To purify AgNWs, the solution was left overnight, then the upper layer was poured out to remove the silver nanoparticles and was replaced with deionized water. The purification was repeated for three times, which led to the final AgNWs aqueous dispersion of a concentration of 24 mg mL^{-1}.

2.3. Preparation of PVA/AgNWs Bilayer Hydrogels

To obtain a conductive, mechanically strong hydrogel sensor, a bilayer structure composed of one layer of strong PVA and one layer of PVA/AgNWs sensing layer was designed as illustrated in **Figure 1**A. The PVA substrate provides a mechanical support for the sensing layer while the top PVA/AgNWs layer offers a piezoresistive capability. The main piezoresistivity mechanism may include the disconnection between AgNWs and increased interparticle distance upon stretching, which leads to increased electrical resistance (Figure 1B).[33] The mechanical property of this bilayer sensor largely depends on the PVA substrate, which can be fabricated by changing the concentration of PVA solution. In the present work, concentrations including 15, 20, 25, and 30 wt% were used. First, PVA powder was added to Milli-Q water with the desired concentrations and subjected to vigorous stirring at 90 °C to dissolve it entirely. Then, the solution was transferred to a Petri dish. The sensing layer was prepared by mixing AgNWs (24 mg mL^{-1}) and PVA (25 wt%) aqueous solution (PVA concentration is 6 wt% in the resultant mixture). Subsequently, the resulting PVA/AgNWs aqueous dispersion was poured directly on top of the pure PVA substrate. The thickness of the two layers was controlled by calculating the volume of the added solution/dispersion. The bilayer assembly was physically cross-linked to form mechanically strong hydrogels using the well-known freezing–thawing method.[29] This involves freezing it to −20 °C for 3 h followed by thawing it at room temperature overnight.

To examine the effects of the concentration of conductive material on the properties of PVA/AgNW hydrogel sensors, four samples were prepared, following the same protocol described above, with different concentrations (24, 18, 12, and 8 mg mL^{-1}) of AgNWs in the sensing layer, while the substrate was PVA of 25 wt%.

2.4. Characterization of the Morphology and Mechanical Properties

The morphology of the synthesized AgNWs was examined using bright field microscopy (CKX53, Olympus) and scanning electron microscopy (SEM, FEI Nova NanoSEM). The microstructure of the sensors was observed by an environmental scanning electron microscope (SEM-TM4000Plus).

To examine the tensile properties of the hydrogels, specimens were cut into strips with dimensions of 40 mm (length) × 6 mm (width) × 2 mm (thickness). All tensile tests were conducted using a tensile testing machine (E42, MTS Systems) at a crosshead speed of 5 mm s^{-1} until samples were ruptured. The rheological properties of the pure PVA substrate and the PVA/AgNWs sensing layer were characterized using an Anton

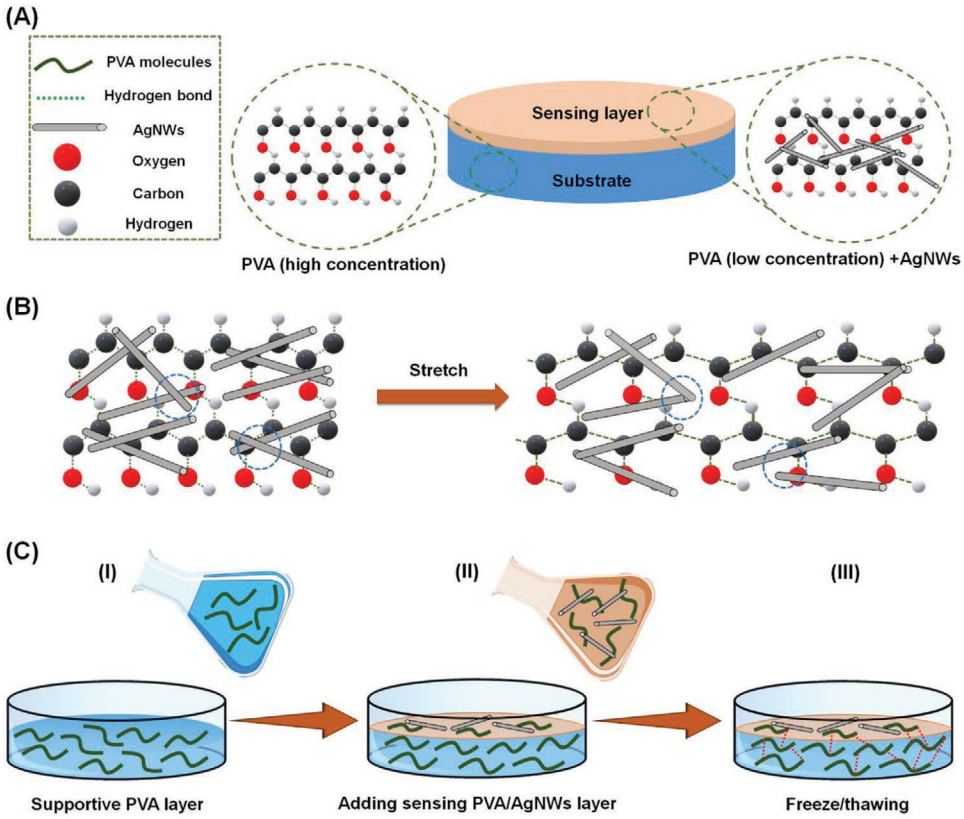

Figure 1. Schematic illustration of the fabrication process and working mechanism of hydrogel strain sensor. A) Design of the bilayer sensor containing the bottom PVA substrate layer and the top PVA/AgNWs sensing layer; B) The main sensing mechanism: disconnection of AgNWs and increased interparticle distance, indicated by the cycles; C) Fabrication procedure: I) Firstly, a substrate layer made of pure PVA hydrogel was fabricated; II) then, a sensing layer (PVA/AgNWs hybrid) was coated on the surface of the PVA substrate; III) the sensor was subjected to one cycle of freezing–thawing.

Paar MCR302 Rheometer with a parallel plate. Four pure PVA samples with different concentrations (15, 20, 25, and 30 wt%) were synthesized and cut into disks with a diameter of 20 mm and a thickness of 2 mm. First, the dynamic amplitude sweep test was conducted over the strain range of 0.001–1000% with constant angular velocity of 10 rad s^{-1} at 25 °C. The storage modulus (G') and loss modulus (G'') were recorded and the amplitude-linear viscoelastic region was determined to select a constant strain for the frequency sweep test.[34] Second, oscillatory frequency sweep measurements were conducted over the frequency range of 0.01–100 Hz with a constant strain of 1%. The storage and loss modulus (G' and G'') were recorded to obtain the frequency-linear viscoelastic range.

2.5. Piezoresistivity Measurements

To measure the piezoresistive properties of the hydrogel sensors, the samples were cut into rectangular shape with dimension of 40 mm (length) × 6 mm (width) × 2 mm (thickness). The electrodes were attached to the two ends of the samples. Electrical resistance of the bilayer PVA/AgNWs samples under mechanical deformation was recorded by a digital multimeter (Keysight LCR meter (model E4980 AL)). Cyclic stretching–releasing was applied to the samples using a custom-made stretching device. For the cyclic loading, all samples were subjected to ten cycles of various peak strains including 50%, 100%, 150%, 200%, and 250% at a strain rate of 0.25 s^{-1}. The relative change in resistance was calculated using the following expression

$$\frac{\Delta R}{R_i} = \frac{R - R_i}{R_i} \tag{1}$$

where R_i and R denote the initial resistance and the resistance at a given mechanical stretch, respectively. The PVA/AgNWs hydrogels were also subjected to monotonic stretching up to breaking strain at a strain rate of 0.25 s^{-1}. The resulting relative resistance change $\Delta R/R_i$ versus strain $\Delta L/L_i$ data were used to calculate the strain sensitivity S (gauge factor)

$$S = \frac{\Delta R/R_i}{\Delta L/L_i} \tag{2}$$

where L_i and L denote the initial length and the instantaneous length of the sensor in the stretched state, respectively.

To investigate the durability of the hydrogel sensors, 2000 cycles of loading–unloading were carried out with a peak strain of 50% at a strain rate of 0.25 s^{-1}. The dependence of the bilayer sensor on the strain rate was investigated through cyclic stretching of the bilayer hydrogel at three different strain rates of 0.25, 0.5, and 0.75 s^{-1}. The response time of the sensor was

examined by rapidly stretching the sensors to a strain of 100% at a ramping rate of 3.0 s^{-1}. The response time was estimated by subtracting the time needed for the stage to reach 100% strain (0.36 s).

2.6. Detecting Human Motion Sensing

As a proof-of-concept, the potential application of the fabricated PVA/AgNWs hydrogel sensor in detecting human joint movements was examined by directly attaching sensors with dimension of 20 mm (length) × 6 mm (width) × 2 mm (thickness) to an index finger, wrist, elbow, and foot using adhesive strips, while the electrodes attached onto the two ends of samples were connected to the digital multimeter for resistance measurement. During the test, the sensor was carefully monitored to ensure good adherence to the skin. The variation of resistance due to the elbow flexion, index finger motion (45° and 90°), wrist bending, and foot flexion was recorded. The same method was used to detect facial expression (the resistance change was measured in response to the folding of forehead and smile). Consent was obtained before the measurements on a human subject.

2.7. Biocompatibility Evaluation of PVA and PVA/AgNWs Hydrogels

The biocompatibility of the hydrogels was assessed through cytotoxicity 3-[4,[5-dimethylthiazol-2-yl]-2,5-diphenyl tetrazolium bromide (MTT) assay to check whether the PVA/AgNWs sensor has the potential to be used as a direct epidermal sensor. Human fibroblasts, the main cellular components of skin, were purchased from Lonza and utilized to examine whether their viability and proliferation change in response to culturing on the PVA and PVA/AgNWs substrate. Fibroblasts were cultured in DMEM (Thermo Fisher Scientific) supplemented with 10% FBS (Thermo Fisher Scientific) in the condition of 37 °C and 5% CO_2. Cells were subcultured at 80% confluency and used at passage 3–5 for cytotoxicity measurements.

The hydrogel substrates cut into disks with a diameter of 7 mm and a thickness of 2 mm. Then, they were placed in a 96-well plate and exposed to UV treatment for sterilization purposes. Subsequently, fibroblasts were detached from the culture flasks using Trypsin (Thermo Fisher Scientific), and centrifuged to reach to the concentration of 5×10^5 cells mL^{-1}. A total number of 7×10^3 cells were added to each hydrogel-containing well, while the same number of cells was seeded in the empty wells (polystyrene) as the control group. The MTT assay was performed according to previously published protocol and the manufacturer's instruction at day 1, 3, 5, and 7 of culture.[35] Briefly, the culture media was removed and 50 µL of MTT solution was added to each well followed by incubating for 3 h at room temperature. Then, 50 µL of stop solution was added to each well and the optical density (OD) that corresponds to the number of viable cells was immediately measured using a spectrophotometer (Biorad microplate reader) at 590 nm. To find the cytotoxicity, the optical density of samples in different days was measured and normalized to the control group (polystyrene well).

To further analyze the cellular morphology, immunostaining of fibroblast cultured on control, PVA, and PVA/AgNWs substrates was performed. Since the PVA-based substrates are not fully transparent, immunostaining enabled the cell morphology assessment. After 24 h of cell seeding among three study groups, cells were fixed with paraformaldehyde for 15 min followed by washing with PBS. Then, to visualize cellular membrane, cells were incubated with CellTracker CM-Dil dye (ThermoFisher Scientific) for 15 min followed by nucleus staining using 4′,6-diamidino-2-phenylindole (DAPI). The stained cells were then used for the fluorescence examination using Olympus FV1000 confocal microscope and Olympus IX83 florescent microscope.

3. Results and Discussion

3.1. Microstructure and Mechanical Properties of the PVA/AgNWs Bilayer Hydrogels

A typical optical microscopy image and SEM image of the synthesized AgNWs are shown in **Figure 2**A,B, respectively. The average length of the AgNWs is estimated to be around 43 µm with the length ranging from 5 to 60 µm while the diameter is ≈100 nm on average. The cross section of the PVA/AgNWs bilayer sensor presented in Figure 2C shows that the sensing layer composed of PVA and AgNWs is very thin (thickness = 15 ± 5 µm) compared to the PVA substrate (thickness = 2 ± 0.1 mm). Therefore, the mechanical properties of the sensor are mainly dictated by the substrate layer. Moreover, a SEM image of the interface of the sensor layer and the substrate in Figure 2E indicates that the two layers were well bonded without any visible delamination. The two layers remain well-bonded even after stretching to 100% strain for multiple cycles (e.g., 20 cycles, as shown in Figure 2F). The method we used to fabricate the bilayer structure resulted in strong bonding between the mechanical supporting substrate and the resistive sensing layer, which avoids delamination upon stretching. In the top view of the sensor shown in Figure 2D, discrete AgNWs can be seen.

The mechanical properties of the PVA/AgNWs bilayer sensor with the substrate made of PVA solution of different concentrations were characterized through tensile testing. The stress–strain curves are shown in **Figure 3**A. The results indicate that the Young's modulus, tensile strength, and stretchability (defined here as the elongation at break) of the hydrogel sensors depend strongly on the PVA concentration. Decreasing the PVA concentration from 30 to 15 wt% resulted in a reduction of the Young's modulus from ≈214 to 22 kPa, as shown in Figure 3B. Moreover, the highly concentrated PVA hydrogels (30 and 25 wt%) exhibited tensile strength of ≈862 and 408 kPa, respectively, which were much higher than that of low PVA concentrations (20 and 15 wt%) with values of ≈163 and 161 kPa, respectively. The results in Figure 3A show that all the PVA/AgNWs hydrogels have a failure strain in the range of 450–550%, indicating their very high stretchability. The stretchability of the sensors seems to decrease as the concentration of PVA in the substrate increases. For example, among the four sensors, the substrate made of a PVA solution of 30 wt%

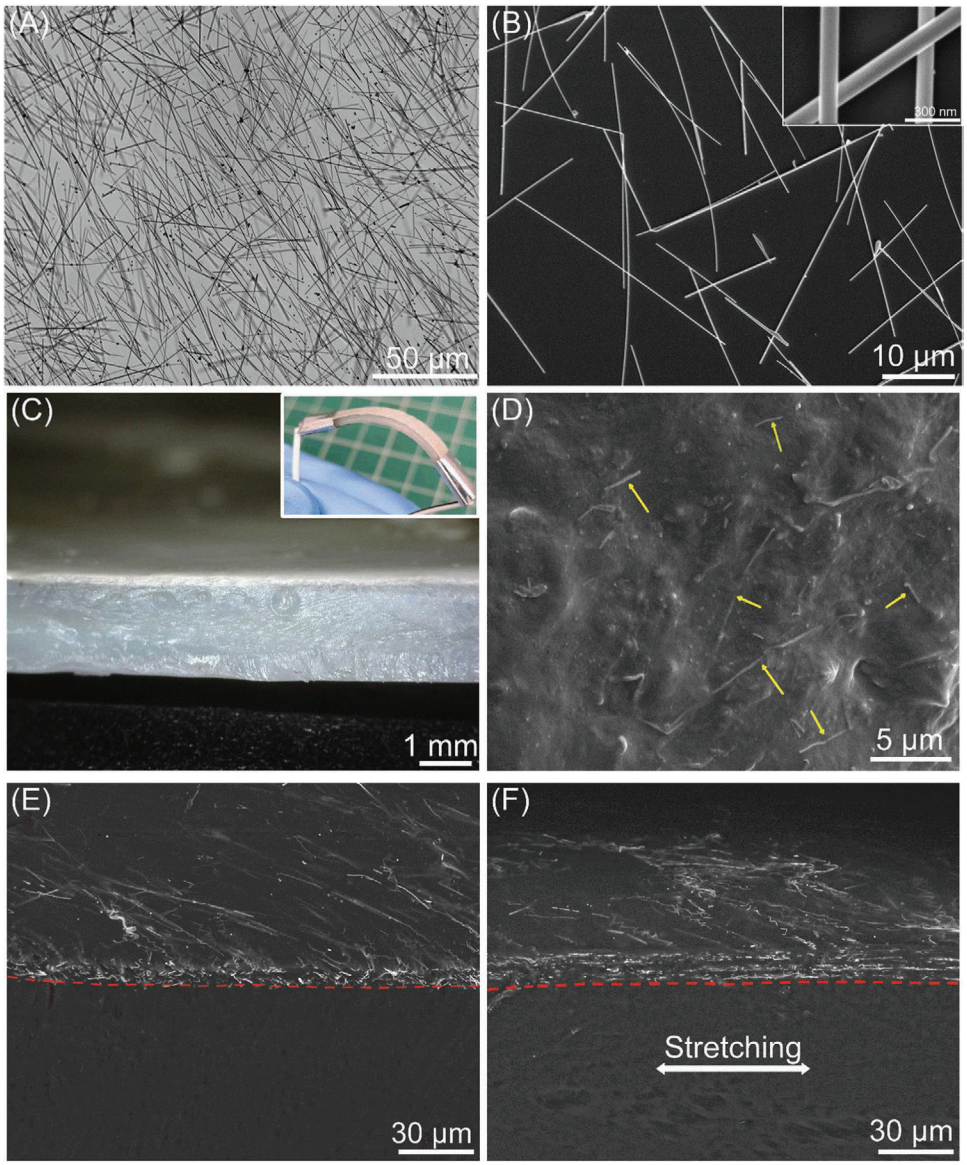

Figure 2. Microstructure of the synthesized AgNWs: A) optical microscopy image and B) SEM image (inset: high-magnification image); Morphology of the fabricated bilayer hydrogel sensor: C) optical microscopy image of the cross section (inset: digital photo of the sensor); D,E) SEM image of the top and cross-section view, respectively; F) the cross-section view of the sensor under stretching to 100% strain. The arrows in (D) indicate the embedded AgNWs. Dashed lines in (E) and (F) indicate the interface of the two layers.

displayed the lowest failure strain of 450%. The PVA concentration is known to influence the mechanical properties of PVA hydrogels.[29,36] These results confirm that the physical cross-linking by the freezing–thawing method can achieve mechanically stable hydrogels without adding extra cross-linking agents.

The mechanical properties of PVA-based conductive composites were further characterized using rheology measurements. The results from frequency sweep and amplitude sweep tests are presented in Figure 3C–E, which show that increasing the concentration of PVA in the substrate layer from 15 to 30 wt% resulted in a higher storage (G') and loss (G'') moduli in the linear viscoelastic regime. These results are in good agreement with a previous report.[37] The linear ranges, defined as the decrease in elastic modulus, are found to be around 100%. For the PVA/AgNWs sensing layer containing PVA 6 wt% and AgNWs 8 mg mL^{-1}, the storage modulus, as shown in Figure 3E, is much lower (a factor of 10) than that pertinent to the substrate made of PVA of 15 wt%.

3.2. Effects of PVA Concentration in the Substrate on the Piezoresistivity of the PVA/AgNWs Bilayer Sensors

Figure 4 displays the piezoresistive responses of the PVA/AgNWs sensors. Figure 4A shows the relative change in the resistance ($\Delta R/R_i$) under monotonic loading while Figure 4B indicates the resistance change under cyclic loading-unloading with different peak strains of 50%, 100%, 150%, 200%, and

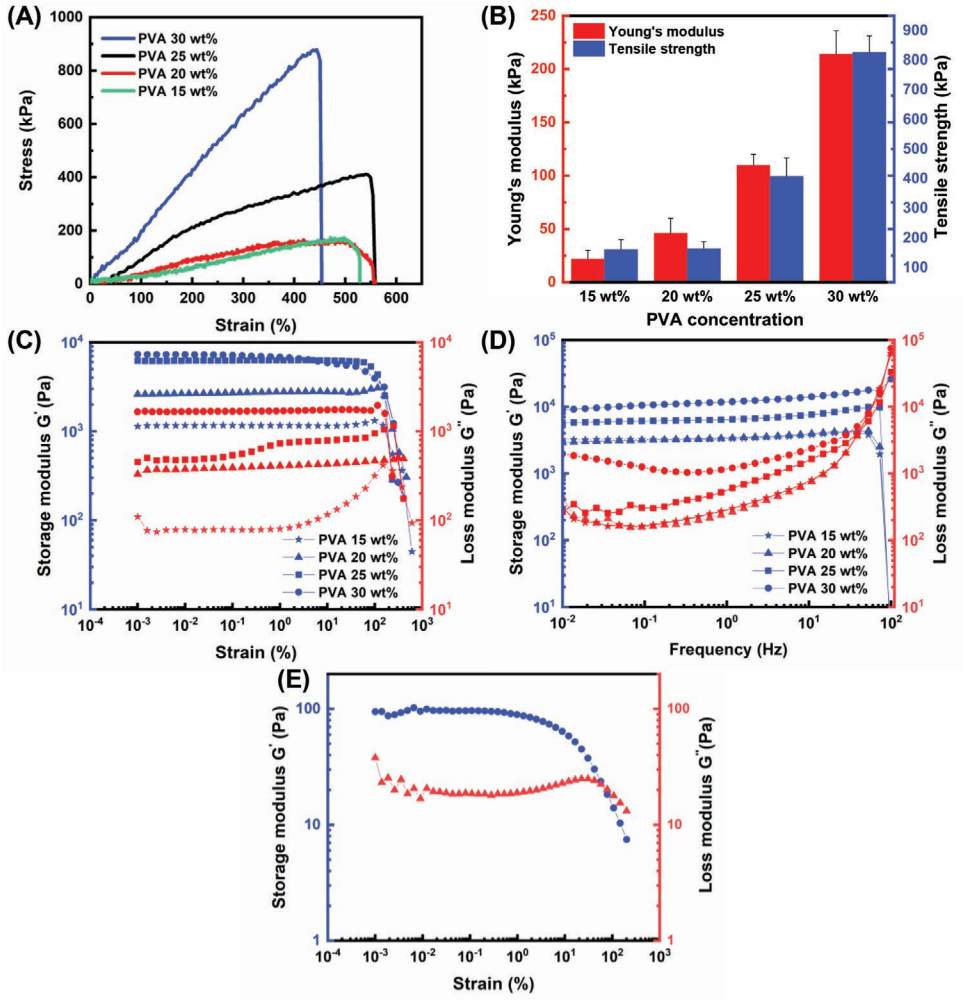

Figure 3. Mechanical properties of PVA/AgNWs bilayer hydrogels. A) Stress–strain curves obtained by monotonic tensile testing; B) the Young's moduli and tensile strengths; storage and loss moduli of hydrogels from PVA solutions of different concentrations obtained from C) amplitude sweep test and D) frequency sweep test; E) storage and loss moduli of the PVA/AgNWs sensing layer.

250%. The results indicate that the sensor resistance gradually increased with stretching and decreased upon unloading with very little hysteresis. The mechanism of this response is related to the change in the conductive network formed by AgNWs in the sensing layer. Stretching increases the distance between nanowires and reduces the overlapping between them, which results in higher resistance (Figure 1B).[16,38,39]

Figure 4A,B indicates that the sensor performance depends on the mechanical properties of the PVA substrate. Changing the PVA concentration from 15 to 25 wt% led to an increase in strain sensitivity (gauge factor increases from 0.1 to 0.34), as shown in Figure 4E. One possible reason for this behavior may be due to the stiffness difference between the sensing layer and the substrate layer. Compared to the substrate layer (15 to 30 wt%), the sensing layer contains a much lower concentration of PVA (6 wt%). The modulus mismatch between the sensing layer and the substrate layers increases by increasing the PVA concentration in the substrate layer. As the substrate becomes stiffer, the shear-lag effect in the load transfer from the substrate to the sensing layer decreases, causing the load in the sensing layer to increase, leading to a higher sensitivity.[40] However, further increasing the PVA concentration to 30 wt% leads to a slight decrease in sensitivity. It should be noted that the top layer is the same in these samples (i.e., composed of PVA of 6 wt% and AgNWs of 18 mg mL^{-1}). All samples exhibited excellent linearity up to 500% strain. This high linearity enables a high accuracy and simple calibration, outperforming many recently reported piezoresistive strain sensors which exhibited a poor linearity at large strains.[4,16,32,39]

3.3. Effects of AgNWs Concentration on the Piezoresistivity of the PVA/AgNWs Bilayer Sensors

The changes in sensors' resistance upon stretching are shown in Figure 4C under monotonic, and Figure 4D under cyclic loading–unloading for sensors containing different concentrations of AgNWs. The gauge factors of the sensors are plotted as a function of the AgNWs concentration in Figure 4F. It is

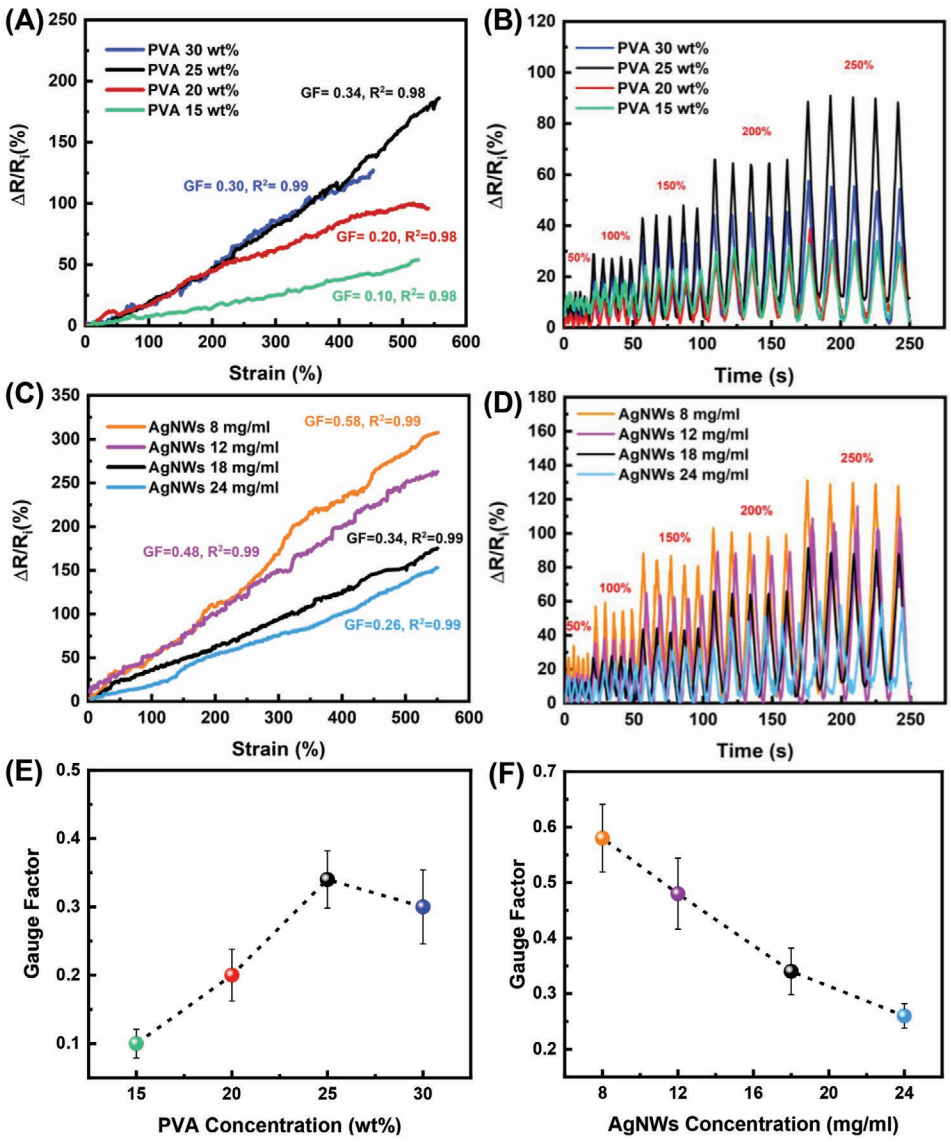

Figure 4. Piezoresistive responses of PVA/AgNWs bilayer composites. A) Relative change in the resistance ($\Delta R/R_i$) when subjected to monotonic stretching for sensors containing different concentrations of PVA in the substrate layer; B) $\Delta R/R_i$ under cyclic loading–unloading with different peak strains from 50% to 250%; C) $\Delta R/R_i$ when subjected to monotonic stretching for sensors with different concentrations of AgNWs in the sensing layer and the co D) $\Delta R/R_i$ under cyclic loading–unloading with different peak tensile strains from 50% to 250%; E,F) the gauge factor versus PVA concentration in the substrate layer and AgNWs concentration in the sensing layer.

interesting to note that the sensor consisting of 8 mg mL^{-1} AgNWs shows the highest sensitivity, and the sensitivity decreases as AgNWs concentration increases. In contrast, the linearity and stretchability of the sensor are not affected by the AgNWs concentration, with all the sensors showing excellent linearity up to 500% strain. As discussed in Section 2.3, the main piezoresistive mechanism may be the changes in the conductive pathways induced by the applied strain, which may include the disconnection between AgNWs and increased interparticle distance upon stretching, as evidenced by **Figure 5**. As indicated by the dashed ovals, some of the initially overlapped AgNWs are disconnected and separated from each other when subjected to stretching, causing the resistance to increase. With a lower concentration of AgNWs, nanowires are overlapping to a lower extent. The conductive pathways are thus easier to be disrupted than those in sensors with higher AgNWs concentration, leading to higher sensitivity. This result is consistent with previous reports.[15,22] It should be noticed that PVA concentration in the substrate was kept at 25 wt% for all these sensors. The electrical conductivities of the sensors made of AgNWs of different concentrations (24, 18, 12, and 6 mg mL^{-1}) are 1.85, 1.38, 1.06, and 0.72 S m^{-1}, respectively. Further decreasing the AgNWs concentration below 8 mg mL^{-1}, e.g., 6 mg mL^{-1}, resulted in samples with very low electrical conductivity which makes the resistance too high to be measured by the commonly used multimeter.

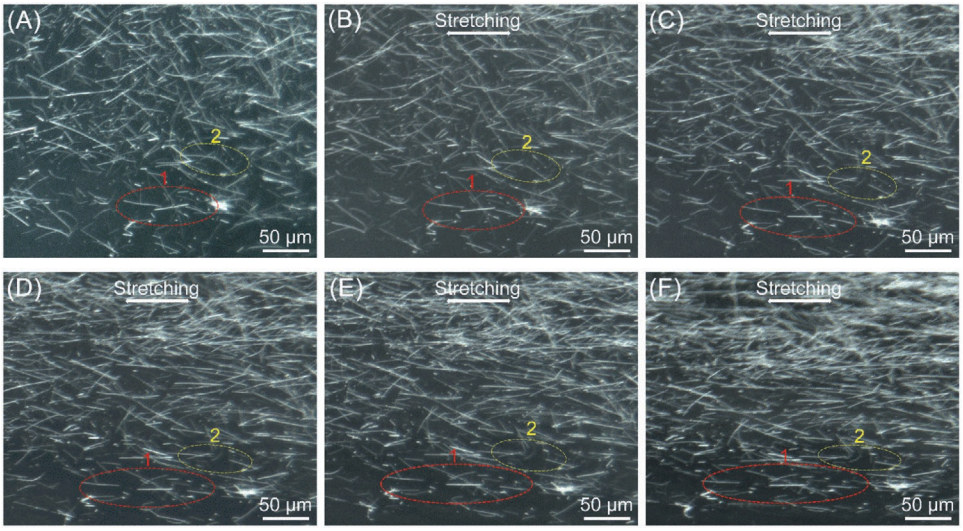

Figure 5. Optical microscopy images of the bilayer PVA/AgNWs hydrogel. A) Without applying any strain; B–F) Under tensile strain of 10%, 30%, 50%, 70%, and 100%.

3.4. PVA/AgNWs Sensor Stability and Response Time

The results presented in the previous sections reveal that the optimal sensing performance was achieved when the substrate contains 25 wt% PVA and the sensing layer contains 8 mg mL^{-1} AgNWs. This optimal sensor design was subsequently used to investigate the stability, durability, and response time as shown in **Figure 6**. First, the fabricated sensor did not show any significant dependency on the strain rate (Figure 6A), indicating that the present sensor can perform stably under different deformation rates.

Furthermore, the optimal sensor design demonstrated a long-term durability without obvious signal degradation when subjected to 2000 cycles at a high peak strain of 50%

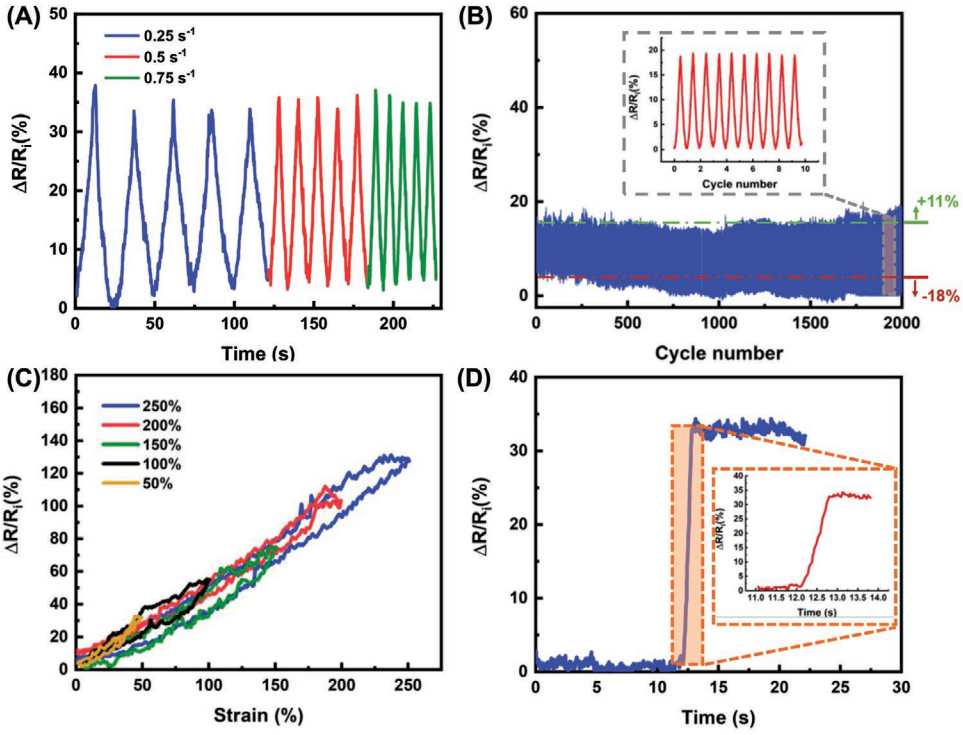

Figure 6. Frequency dependency, durability, and response time of the PVA/AgNWs sensor. A) Relative change in the resistance ($\Delta R/R_i$) when subjected to stretching–releasing at different strain rates (the peak strain is 100%); B) $\Delta R/R_i$ under 2000 cycles of stretching–releasing (the peak strain is 50%); C) $\Delta R/R_i$ versus strain curves when subjected to cyclic stretching–releasing; D) the response time of the sensor when stretched to 100% strain at a strain rate of 3.0 s^{-1}.

(Figure 6B). During the first 1000 cycles, there was a slight downward drift in the peak value of $\Delta R/R_i$, followed by a slight upward drift after 1000 cycles. Around 11–18% change (as indicated in Figure 6B) in the sensor response was observed under 2000 cycles (the peak value of $\Delta R/R_i$ increased by around 0.005% cycle^{-1}, and the initial resistance decreased by ≈0.009% cycle^{-1}). There was also minor fluctuation in the signals although the enlarged detail in Figure 6B exhibited good reproducibility. This slight drift may be attributed to the evaporation of water in the hydrogel-based sensors.[16,17,38] In addition, the small hysteresis of the sensor, as discussed later, could also lead to the signal drift.[16] Nevertheless, the results show that PVA/AgNWs sensor has an excellent durability up to 2000 cycles, comparable to a previous report.[38] The remarkably stable performance of present sensor confirms its high potential for practical applications such as wearable sensors for long-term monitoring.

One of the main metrics for a strain sensor is the hysteresis behavior. The piezoresistive sensors based on polymer nanocomposites usually suffer from high hysteresis, which is believed to be caused by the viscoelasticity of the polymer matrix and by the rearrangement of the conductive nanomaterials in the matrix.[16,20,41] As a consequence, the resistance changes of the embedded conductive network within the polymer matrix are also time-dependent. For instance, a significant hysteresis has been reported for a polyacrylamide-based strain sensor with gauge factor of 0.63 at 1000% strain.[42] Here, the hysteresis behavior of PVA/AgNWs sensor at a wide range of strain from 50% to 250% for the strain rate of 0.25 s^{-1} is shown in Figure 6C. Hysteresis can be quantitatively estimated according to our previous work.[43] An average hysteresis value of 7% ± 0.5% was calculated based on Figure 6C. A small hysteresis in electrical response of sensor confirms its high potential in quickly responding to stretching. This behavior may be related to the strong binding between substrate and the sensing layer.

Response time is also a critical parameter, which directly affects the practical applications of devices in dynamic and continuous monitoring of strain. Figure 6D indicates the response time of PVA/AgNWs sensor when it was subjected to a rapid stretching to a strain of 100% at a strain rate of 3.0 s^{-1}. At this strain rate, it takes 0.36 s for the sensor to reach the target strain. Since the jump in sensor response shown in Figure 6D

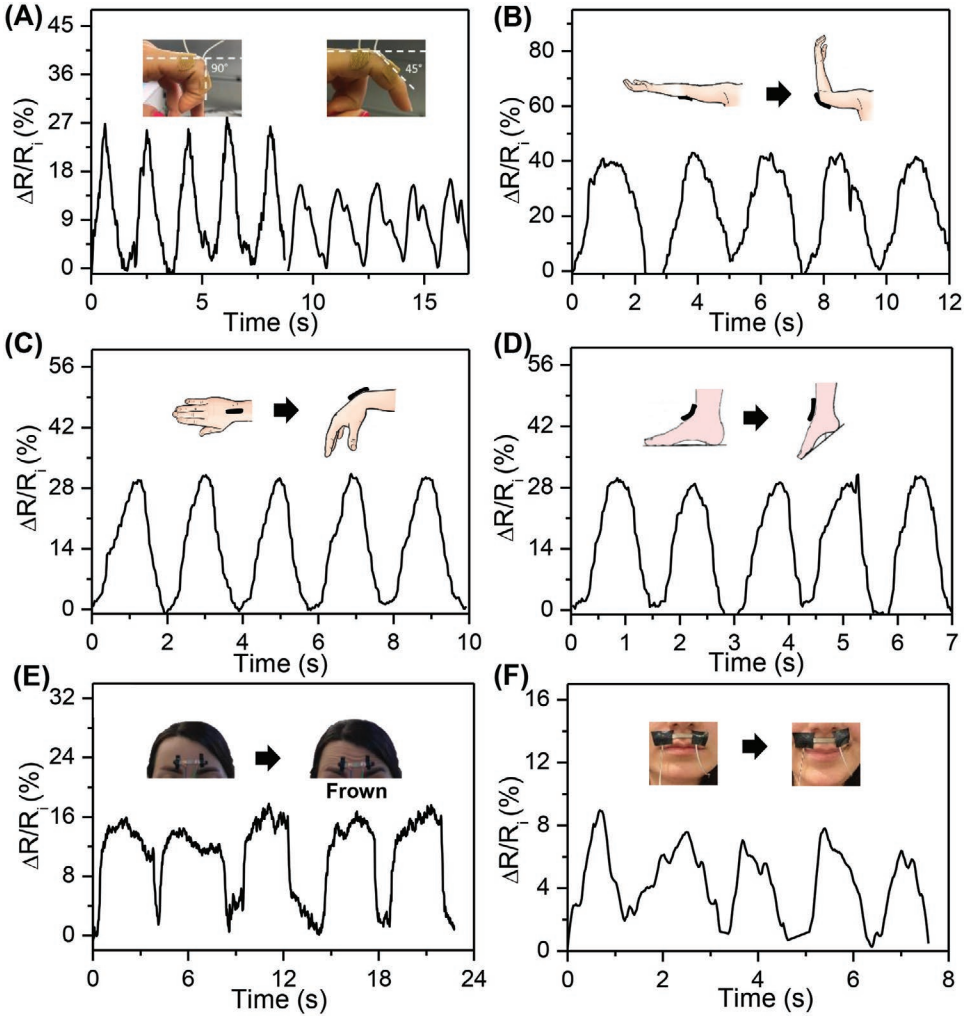

Figure 7. Detecting human motions using the bilayer PVA/AgNWs sensor. Relative change in the resistance ($\Delta R/R_i$) induced by bending of A) index finger, B) elbow, C) wrist, D) foot, E) forehead folding, and F) smile.

occurred over a time of 0.68 s, the latency or response time of the sensor is estimated to be 0.32 s, which indicates a very rapid response.

3.5. Application Demonstration

Having confirmed the stability, linearity, and rapid response of the strain sensors based on conductive hydrogels developed in this study, a demonstration is present below to show the sensors' potential for application as wearable sensors. Sensors with the highest sensitivity (25 wt% PVA in the substrate layer and 8 mg mL^{-1} AgNWs in the sensing layer) were used to investigate their ability in detecting human motions including joint movements and facial expression. **Figure 7**A shows that the sensor can detect the bending of finger joints with greater increase in the resistance being observed when subjected to larger degree of bending. Bending the finger to angles of 90° and 45° resulted in ≈27%, and 14% change in resistance, indicating ≈46%, and 24% strain were induced, respectively, which agrees well with our previous work.[43] Moreover, the sensor can also respond to the bending of elbow (Figure 7B), wrist (Figure 7C), and foot (Figure 7D) joints. The maximum strain measured was around 68% for elbow bending and ≈48% for wrist and foot bending, in good agreement with a previous report.[44] The sensor exhibits a very high stability as no visible damage was observed after the bending cycles. Moreover, the sensor can respond to small deformations of skin induced by forehead folding and smile (Figure 7E,F). These results demonstrate that the bilayer PVA/AgNWs sensor is a promising candidate for wearable electronic devices.

3.6. Biocompatibility of the PVA/AgNWs Sensors

The biocompatibility of the sensors was investigated by using the protocol presented in Section 2.6. The sensors were used as a biological substrate for culturing fibroblasts. To analyze whether fibroblast can easily attach and spread on the PVA-based substrates, cell morphology was investigated after 24 h of cell seeding. **Figure 8**A indicates that immunostained fibroblasts exhibited a well-spread morphology in conventional cell

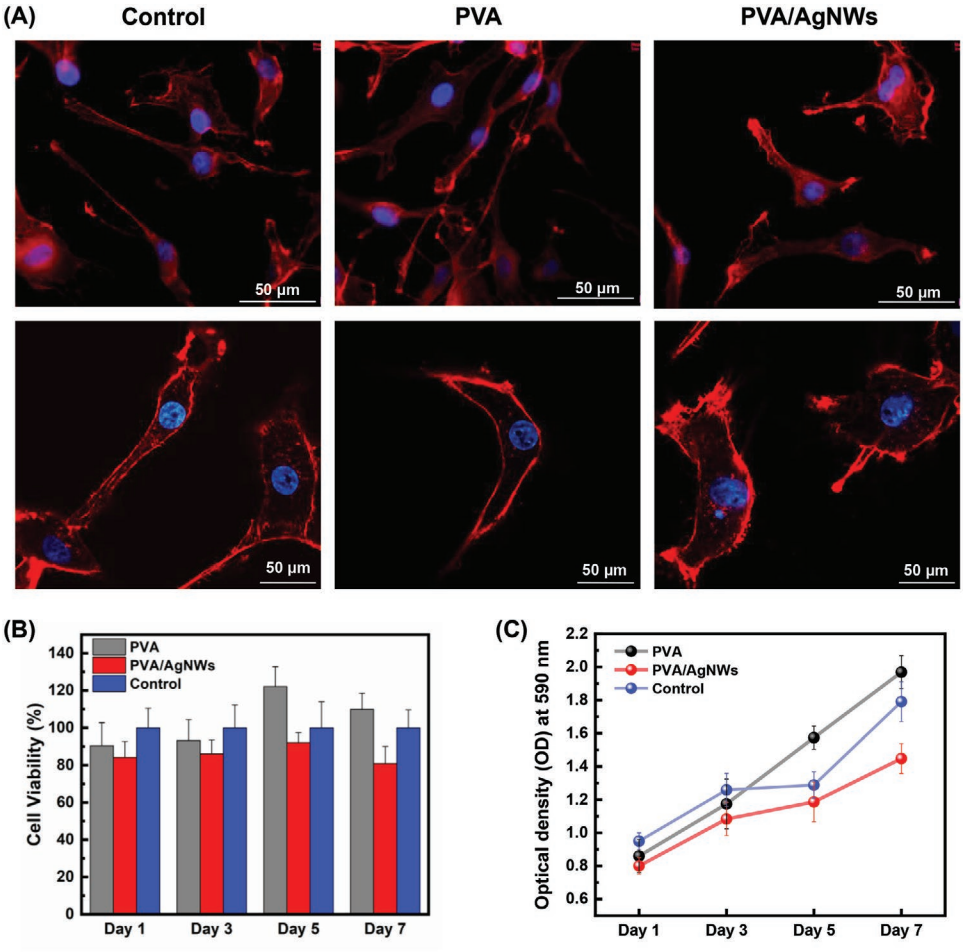

Figure 8. Biocompatibility assessment of PVA-based sensors with fibroblasts. A) Fluorescent images of morphology fibroblasts cultured on control (polystyrene), PVA, and PVA/AgNWs substrates captured by fluorescent microscope (upper panel) and confocal microscope (lower panel); B) normalized cellular viability against PVA, PVA/AgNWs, and polystyrene (control) substrates at day 1, 3, 5, and 7 of culturing fibroblasts; C) the OD values from day 1 to 7 in three study groups (PVA, PVA/AgNWs, and control) confirm the successful cell proliferation.

culture substrates (polystyrene) as well as both PVA and PVA/AgNWs substrates. Since fibroblasts are a type of adherent cells, they are required to attach to the substrate and spread to achieve biological functions such as proliferation and differentiation. While cells showed more elongated morphology on the polystyrene substrates, they could successfully attach and spread on PVA and PVA/AgNWs substrates. Moreover, the cytotoxicity and proliferation were assessed at day 1, 3, 5, and 7 time points of cell culturing (Figure 8B). Cytotoxicity measurements showed that the developed hydrogels did not affect the cellular viability and proliferation. Figure 8B indicates the cytotoxicity measurements of fibroblasts in three study groups of PVA, PVA/AgNWs, and control (polystyrene). The OD values were normalized against the control group in each day. The normalized OD values in PVA and PVA/AgNWs groups did not show a significant difference as compared to the control group which confirmed that the mentioned substrate did not exhibit significant cytotoxic effects against fibroblasts during 7 d of culture. OD value is proportional to the number of viable cells. The increased OD values from day 1 to 7 in all study groups confirm their successful proliferation (Figure 8C). More interestingly, PVA substrate promoted the proliferation of fibroblasts, which resulted in higher OD values at day 4 and 7 comparing to the control group. These results demonstrate that the PVA/AgNWs sensors possess good biocompatibility and they are a promising candidate as a wearable device suitable for direct contact with the skin.

4. Conclusion

In this study, a highly stretchable hydrogel strain sensor has been developed using a bilayer design, i.e., a PVA/AgNWs sensing layer being supported by a pure strong PVA hydrogel substrate. This new type of piezoresistive sensors are mechanically strong, electrically conductive, and featuring excellent linearity up to 500% strain as well as low hysteresis. The sensor sensitivity depends on the stiffness of the PVA hydrogel substrate and the AgNWs concentration in the sensing layer, with the highest sensitivity (a gauge factor of 0.58) observed for the sensor with a substrate made of 25 wt% PVA solution and a sensing layer containing AgNWs of 8 mg mL^{-1}. Moreover, with a strong bonding between the sensing layer and the substrate, the hydrogel-based strain sensor demonstrates high stability with low hysteresis effects. In addition, the PVA/AgNWs hydrogel sensor shows excellent biocompatibility, which makes them suitable for biomedical wearable applications where a direct contact with the skin is required. The sensor has been demonstrated to successfully detect a wide range of human motions such as the bending motion of finger, wrist, and elbow and facial expression. Therefore, this highly stretchable and biocompatible strain sensor has the potential to be used in a wide range of wearable applications.

Acknowledgements

S.W. and S.P. would like to thank the Australian Research Council for financial support through Discovery Early Career Researcher Award (DE170100284, DE190100311).

Conflict of Interest

The authors declare no conflict of interest.

Keywords

biocompatibility, human motion detection, hydrogel strain sensors, polyvinyl alcohol

Received: May 3, 2020
Revised: July 9, 2020
Published online: September 6, 2020

[1] D. H. Kim, N. Lu, R. Ma, Y. S. Kim, R. H. Kim, S. Wang, J. Wu, S. M. Won, H. Tao, A. Islam, K. J. Yu, T. I. Kim, R. Chowdhury, M. Ying, L. Xu, M. Li, H. J. Chung, H. Keum, M. McCormick, P. Liu, Y. W. Zhang, F. G. Omenetto, Y. Huang, T. Coleman, J. A. Rogers, *Science* **2011**, *333*, 838.
[2] D. H. Ho, Q. Sun, S. Y. Kim, J. T. Han, D. H. Kim, J. H. Cho, *Adv. Mater.* **2016**, *28*, 2601.
[3] S. Wu, S. Peng, Z. J. Han, H. Zhu, C. H. Wang, *ACS Appl. Mater. Interfaces* **2018**, *10*, 36312.
[4] F. Zhang, H. Hu, M. Islam, S. Peng, S. Wu, S. Lim, Y. Zhou, C.-H. Wang, *Compos. Sci. Technol.* **2019**, 107959.
[5] Q. Jiang, C. Tang, H. Wang, J. Yang, J. Li, C. Gu, G. Yu, *Adv. Mater. Technol.* **2019**, *4*, 1800572.
[6] P. Wei, X. Yang, Z. Cao, X.-L. Guo, H. Jiang, Y. Chen, M. Morikado, X. Qiu, D. Yu, *Adv. Mater. Technol.* **2019**, *4*, 1900315.
[7] S. H. Peng, P. Blanloeuil, S. Y. Wu, C. H. Wang, *Adv. Mater. Interfaces* **2018**, *5*, 1800403.
[8] Y. Jiang, M. Liu, X. Yan, T. Ono, L. Feng, J. Cai, D. Zhang, *Adv. Mater. Technol.* **2018**, *3*, 1800113.
[9] Y. Xia, Y. Wu, T. Yu, S. Xue, M. Guo, J. Li, Z. Li, *ACS Appl. Mater. Interfaces* **2019**, *11*, 21117.
[10] M. A. Raoufi, S. A. Moshizi, A. Razmjou, S. Y. Wu, M. E. Warkiani, M. Asadnia, *IEEE Sens. J.* **2019**, *19*, 11675.
[11] A. G. P. Kottapalli, M. Asadnia, J. Miao, M. Triantafyllou, *J. Intell. Mater. Syst. Struct.* **2015**, *26*, 38.
[12] S. A. Moshizi, S. Azadi, A. Belford, A. Razmjou, S. Wu, Z. J. Han, M. Asadnia, *Nano-Micro Lett.* **2020**, *12*, 109.
[13] W. Lan, Y. X. Chen, Z. W. Yang, W. H. Han, J. Y. Zhou, Y. Zhang, J. Y. Wang, G. M. Tang, Y. P. Wei, W. Dou, Q. Su, E. Q. Xie, *ACS Appl. Mater. Interfaces* **2017**, *9*, 6644.
[14] F. Ejeian, S. Azadi, A. Razmjou, Y. Orooji, A. Kottapalli, M. E. Warkiani, M. Asadnia, *Sens. Actuators, A* **2019**, *295*, 483.
[15] S. Wu, J. Zhang, R. B. Ladani, A. R. Ravindran, A. P. Mouritz, A. J. Kinloch, C. H. Wang, *ACS Appl. Mater. Interfaces* **2017**, *9*, 14207.
[16] G. Cai, J. Wang, K. Qian, J. Chen, S. Li, P. S. Lee, *Adv. Sci.* **2017**, *4*, 1600190.
[17] H. Zhang, W. Niu, S. Zhang, *ACS Appl. Mater. Interfaces* **2018**, *10*, 32640.
[18] H. Khan, A. Razmjou, M. E. Warkiani, A. Kottapalli, M. Asadnia, *Sensors* **2018**, *18*, 418.
[19] S. Peng, S. Wu, F. Zhang, C. H. Wang, *Adv. Mater. Technol.* **2019**, *4*, 1900060.
[20] N. Wang, Z. Y. Xu, P. F. Zhan, K. Dai, G. Q. Zheng, C. T. Liu, C. Y. Shen, *J. Mater. Chem. C* **2017**, *5*, 4408.
[21] S. Wu, R. B. Ladani, J. Zhang, K. Ghorbani, X. Zhang, A. P. Mouritz, A. J. Kinloch, C. H. Wang, *ACS Appl. Mater. Interfaces* **2016**, *8*, 24853.
[22] M. Amjadi, A. Pichitpajongkit, S. Lee, S. Ryu, I. Park, *ACS Nano* **2014**, *8*, 5154.

[23] L.-W. Lo, H. Shi, H. Wan, Z. Xu, X. Tan, C. Wang, *Adv. Mater. Technol.* **2020**, *5*, 1900717.
[24] X. Q. Li, Y. J. Jiang, F. Wang, Z. J. Fan, H. N. Wang, C. H. Tao, Z. F. Wang, *RSC Adv.* **2017**, *7*, 46480.
[25] Q. Zhang, X. Liu, L. J. Duan, G. H. Gao, *Chem. Eng. J.* **2019**, *365*, 10.
[26] Z. Wang, H. Zhou, J. Lai, B. Yan, H. Liu, X. Jin, A. Ma, G. Zhang, W. Zhao, W. Chen, *J. Mater. Chem. C* **2018**, *6*, 9200.
[27] X. Pei, H. Zhang, Y. Zhou, L. Zhou, J. Fu, *Mater. Horiz.* **2020**, *7*, 1872.
[28] Y. Zhao, Z. Li, S. Song, K. Yang, H. Liu, Z. Yang, J. Wang, B. Yang, Q. Lin, *Adv. Funct. Mater.* **2019**, *29*, 1901474.
[29] H. J. Zhang, H. S. Xia, Y. Zhao, *ACS Macro Lett.* **2012**, *1*, 1233.
[30] Y. Zhu, W. Lu, Y. Guo, Y. Chen, Y. Wu, H. Lu, *RSC Adv.* **2018**, *8*, 36999.
[31] M. Liao, P. Wan, J. Wen, M. Gong, X. Wu, Y. Wang, R. Shi, L. Zhang, *Adv. Funct. Mater.* **2017**, *27*, 1703852.
[32] X. G. Yu, Y. Q. Li, W. B. Zhu, P. Huang, T. T. Wang, N. Hu, S. Y. Fu, *Nanoscale* **2017**, *9*, 6680.
[33] S. Wu, S. Peng, Y. Yu, C. H. Wang, *Adv. Mater. Technol.* **2020**, *5*, 1900908.
[34] H. Y. Bian, L. Q. Wei, C. X. Lin, Q. L. Ma, H. Q. Dai, J. Y. Zhu, *ACS Sustainable Chem. Eng.* **2018**, *6*, 4821.
[35] E.-E. Hago, X. S. Li, *Adv. Mater. Sci. Eng.* **2013**, *2013*, 328763.
[36] A. Kumar, S. S. Han, *Int. J. Polym. Mater.* **2017**, *66*, 159.
[37] R. Hernández, A. Sarafian, D. López, C. J. P. Mijangos, *Polymer* **2004**, *45*, 5543.
[38] S. Xia, S. Song, F. Jia, G. Gao, *J. Mater. Chem. B* **2019**, *7*, 4638.
[39] X. Jing, H. Y. Mi, Y. J. Lin, E. Enriquez, X. F. Peng, L. S. Turng, *ACS Appl. Mater. Interfaces* **2018**, *10*, 20897.
[40] C. N. Duong, C. H. Wang, in *Composite Repair* (Eds: C. N. Duong, C. H. Wang), Elsevier Science, Oxford **2007**, p. 16.
[41] Y. Lu, M. C. Biswas, Z. Guo, J. W. Jeon, E. K. Wujcik, *Biosens. Bioelectron.* **2019**, *123*, 167.
[42] S. Liu, L. Li, *ACS Appl. Mater. Interfaces* **2017**, *9*, 26429.
[43] S. Wu, S. Peng, C. H. Wang, *Sens. Actuators, A* **2018**, *279*, 90.
[44] A. Morteza, Y. Y. Jin, P. Inkyu, *Nanotechnology* **2015**, *26*, 375501.